Origin of Syrinx Fluid in Syringomyelia: A Physiological Study

John D. Heiss, MD*
Katie Jarvis, MD*
René K. Smith, RN, BSN*
Eric Eskioglu, MD§
Mortimer Gierthmuehlen, MD¶
Nicholas J. Patronas, MD‡
John A. Butman, MD, PhD‡
Davis P. Argersinger, BS*
Russell R. Lonser, MD*
Edward H. Oldfield, MD*†

*Surgical Neurology Branch, NINDS, National Institutes of Health, Bethesda, Maryland; ‡Department of Radiology, Clinical Center, National Institutes of Health, Bethesda, Maryland; §Novant Health Neurosurgery Specialists, Charlotte, North Carolina; ¶Department of Neurosurgery, University of Freiburg, Faculty of Medicine, Freiburg, Germany

†Deceased

Correspondence:
John D. Heiss, MD,
Surgical Neurology Branch, NINDS, NIH,
10 Center Drive, Building 10, Room 3D20, MSC-1414,
Bethesda, MD 20892-1414.
E-mail: heissj@ninds.nih.gov

Received, June 20, 2017.
Accepted, February 13, 2018.
Published Online, March 30, 2018.

BACKGROUND: The origin of syrinx fluid is controversial.
OBJECTIVE: To elucidate the mechanisms of syringomyelia associated with cerebrospinal fluid pathway obstruction and with intramedullary tumors, contrast transport from the spinal subarachnoid space (SAS) to syrinx was evaluated in syringomyelia patients.
METHODS: We prospectively studied patients with syringomyelia: 22 with Chiari I malformation and 16 with SAS obstruction-related syringomyelia before and 1 wk after surgery, and 9 with tumor-related syringomyelia before surgery only. Computed tomography-myelography quantified dye transport into the syrinx before and 0.5, 2, 4, 6, 8, 10, and 22 h after contrast injection by measuring contrast density in Hounsfield units (HU).
RESULTS: Before surgery, more contrast passed into the syrinx in Chiari I malformation-related syringomyelia and spinal obstruction-related syringomyelia than in tumor-related syringomyelia, as measured by (1) maximum syrinx HU, (2) area under the syrinx concentration-time curve (HU AUC), (3) ratio of syrinx HU to subarachnoid cerebrospinal fluid (CSF; SAS) HU, and (4) AUC syrinx/AUC SAS. More contrast (AUC) accumulated in the syrinx and subarachnoid space before than after surgery.
CONCLUSION: Transparenchymal bulk flow of CSF from the subarachnoid space to syrinx occurs in Chiari I malformation-related syringomyelia and spinal obstruction-related syringomyelia. Before surgery, more subarachnoid contrast entered syringes associated with CSF pathway obstruction than with tumor, consistent with syrinx fluid originating from the subarachnoid space in Chiari I malformation and spinal obstruction-related syringomyelia and not from the subarachnoid space in tumor-related syringomyelia. Decompressive surgery opened subarachnoid CSF pathways and reduced contrast entry into syringes associated with CSF pathway obstruction.

KEY WORDS: Syringomyelia, Chiari malformation type 1, Intramedullary spinal tumor, Myelography

Neurosurgery 84:457–468, 2019 DOI:10.1093/neuros/nyy072 www.neurosurgery-online.com

The origin of syrinx fluid associated with obstruction of the subarachnoid cerebrospinal fluid (CSF) pathways is controversial, as is the mechanism for resolution of syringomyelia after surgery. We sought to establish the origin of syrinx fluid in various types of syringomyelia and to explain the mechanism of syrinx resolution that occurs after surgery to eliminate subarachnoid CSF obstruction, at the foramen magnum with the Chiari I malformation and in the spinal subarachnoid space (SAS) in SAS obstruction-related syringomyelia.

ABBREVIATIONS: AUC, area of HU under the concentration-time curve; **Ch-S,** syringomyelia associated with Chiari I malformation; **CSF,** cerebrospinal fluid; **CT,** computed tomography; **HU,** Hounsfield units; **MRI,** magnetic resonance imaging; **SAS,** spinal subarachnoid space; **Sp-S,** spinal subarachnoid space obstruction-related syringomyelia; **Tum-S,** syringomyelia associated with intramedullary hemangioblastomas

Patients with syringomyelia associated with Chiari I malformation (Ch-S), spinal subarachnoid space obstruction (Sp-S), or intramedullary hemangioblastomas (Tum-S) were evaluated using computed tomography (CT) myelography to measure the amount of contrast that would pass over time from the SAS to syringes of various etiologies.[1] Low molecular weight myelogram dye acts as a marker of the movement of CSF. Our hypothesis was that syringomyelia related to obstruction of the CSF pathways develops from accumulation

of CSF that travels through the spinal cord and into the syrinx via an active process, bulk flow.[2-5] In contrast, hemangioblastoma-related syringomyelia results from the vascular permeability of the tumor vessels and intramedullary accumulation of fluid produced by the tumor.[6,7] Thus, the latter group serves as a control for the effects of (1) dye moving into the syrinx by diffusion and bulk flow under physiological conditions and (2) dye entering the syrinx from the vascular system after it is absorbed from the subarachnoid space.[8] If our hypothesis is correct, more dye (CSF) from the subarachnoid space would enter the syrinx in patients with Ch-S or Sp-S than in patients with Tum-S. If the obstruction of subarachnoid CSF pathways is responsible for CSF transport into the syrinx via bulk flow, relief of the obstruction should reduce the amount of contrast that enters the syrinx after compared to before surgery.

METHODS

Study Protocol

From June 1998 to January 2008, 47 patients, 22 men and 25 women, mean age 37 ± 11 yr (range 19-62 yr) with Ch-S (22 patients), Sp-S (6 spinal trauma, 8 focal arachnoiditis, 2 arachnoid cysts), and Tum-S (9 patients with von Hippel-Lindau disease and spinal hemangioblastoma) were enrolled in the clinical research protocol. The protocol for the study received prior approval by the site's institutional review board and radiation safety committee. Study subjects were informed in writing that the CT myelograms were performed for research purposes, involved radiation risk, were necessary to obtain the research information desired, and that the knowledge obtained from the research may not benefit them. Risks of myelography and CT scanning were described in the Informed Consent Document, including the most often reported adverse effects of headache, nausea, vomiting, pain in the back, leg, and neck, and hypotension. Myelography was performed in patients with syringomyelia and without acute signs of cerebellar herniation. Patients were informed that they would stay in the hospital for 24 h after the procedure for observation and for treatment of any side effects of the myelogram dye. Informed consent was obtained from each subject. Chiari I malformation was defined as displacement of the cerebellar tonsils at least 5 mm inferior to the foramen magnum (mean 12 ± 6 mm, range 5-23 mm) associated with impaction of the cerebellar tonsils in the foramen magnum. Patients with Sp-S had at least a partial myelographic block of the subarachnoid space at the level of focal arachnoid adhesions.[2]

All patients received a single CT cut at the spinal level of the greatest expansion of the syrinx before, and 0.5, 2, 4, 6, 8, 10, and 22 h after the injection. At myelography 10 mL of CSF was removed, and 10 mL of water soluble myelogram dye (Isovue-M 300, Bracco Diagnostics Inc, Monroe Township, New Jersey) containing 300 mg/mL of organically bound iodine was injected into the CSF in the SAS under fluoroscopic control. The surgical procedure with Ch-S and Sp-S relieved the block of the subarachnoid space, but did not open the syrinx. These patients underwent CT myelography before and 1 wk after surgery, when magnetic resonance imaging (MRI) demonstrated that the syrinx was the same size as it had been before surgery (ie, the syrinx had not yet had time to collapse after surgery). Myelography was not performed after surgery in the Tum-S group because their syringes had been opened into the subarachnoid CSF at surgery. A computer workstation was used to measure the Hounsfield unit (HU) in the subarachnoid space and syrinx. The change in HU in these structures attributable to dye was calculated by subtracting baseline (before dye injection) HU from values obtained after intrathecal contrast injection. To calibrate HU values to contrast concentration, dilutions of myelogram dye in artificial CSF were CT scanned, displayed graphically, and subjected to linear regression, demonstrating a linear relationship of 29.4 HUs per 1 mg iodine/mL CSF ($r^2 = 0.999$).[9]

Imaging

Midsagittal T1- and T2-weighted MRI with and without contrast of the posterior fossa and spine was evaluated. Syringomyelia was diagnosed by the presence of intramedullary T1 signal hypointensity and T2 signal hyperintensity extending over more than 1 spinal segment that distended the spinal cord. The maximum anteroposterior width and length of the syrinx were measured. The length of the syrinx was recorded in spinal segments (a vertebral body and intervertebral disc). Focal contrast enhancement identified an intramedullary hemangioblastoma in patients with von-Hippel Lindau disease.

Surgery

For Ch-S patients, surgery included suboccipital craniectomy, C1 laminectomy, opening the dura leaving the arachnoid intact, and duraplasty using an autograft of occipital pericranium.[10] For patients with Sp-S, a laminectomy was centered over the region of obstruction, the dura was opened, lesions obstructing the subarachnoid space were removed, and an expansile duraplasty was performed.[3] For patients with Tum-S, a laminectomy was centered over the tumor, the tumor was removed using standard microsurgical techniques, and the dura was closed primarily.[11]

Postoperative Imaging

Patients in the Ch-S and Sp-S groups underwent midsagittal spinal T1-weighted MRI 1 wk after surgery.

Statistical Analysis

The unpaired *t* test was used to evaluate differences between groups (Ch-S, Sp-S, Tum-S). The paired *t* test was used to compare values within the Ch-S and Sp-S groups before and after surgery. Data are mean ± standard deviation. A *P*-value of $\leq .05$ was considered significant. Data were recorded in a spreadsheet (Excel, Microsoft Corp, Redmond, Washington), and statistical analyses were performed using Graphpad Prism (Graphpad Software Inc, La Jolla, California).

One patient with an intramedullary hemangioblastoma had a much higher concentration of contrast in the syrinx than the other members of the Tum-S group. As well as having an intramedullary tumor and syrinx, because of previous spinal surgery at a level cephalad to the current tumor this patient had a myelographic partial subarachnoid block typical of patients in the Sp-S group. Because we could not determine if the very high concentration of contrast in his syrinx was a result of the block of the SAS, rather than the intramedullary tumor, and as his preoperative maximum HU value in the syrinx was >8 standard deviations greater than the mean of the other 8 patients in that group, his values are not included in the calculations.

RESULTS

Representative patients in each group are shown in Figures 1–3. The results of analysis of groups are displayed in Figure 4. No

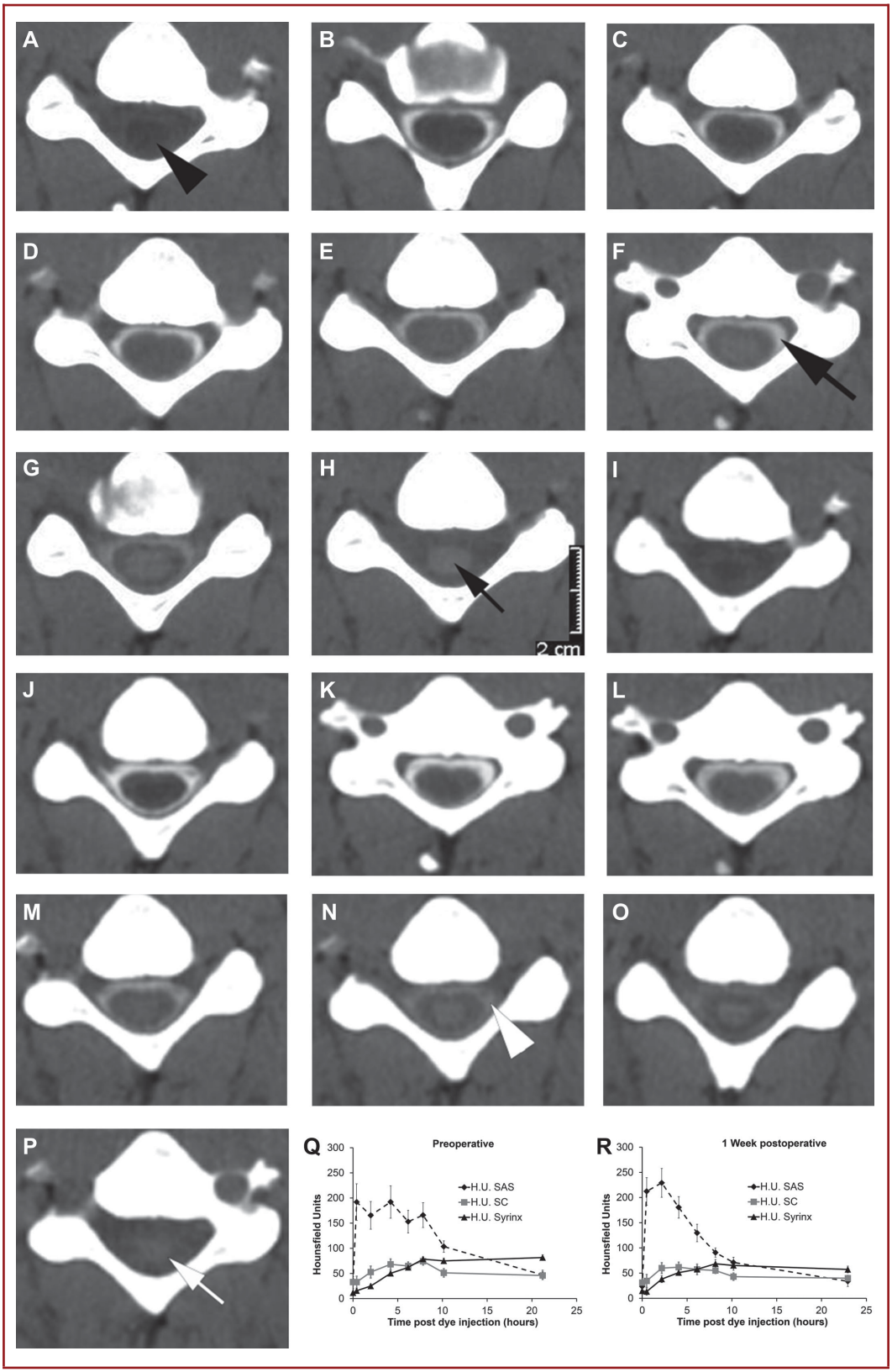
A
B
C
D
E
F
G
H
2 cm
I
J
K
L
M
N
O
P
Q
Preoperative
Hounsfield Units
Time post dye injection (hours)
H.U. SAS
H.U. SC
H.U. Syrinx
R
1 Week postoperative
Hounsfield Units
Time post dye injection (hours)
H.U. SAS
H.U. SC
H.U. Syrinx

FIGURE 1. **A-P**, *Serial CT axial images at the C6 spinal segment before* **A** *through* **H** *and after* **I** *through* **P** *craniocervical decompression for a patient with Chiari I malformation associated with cervicothoracic syringomyelia. Images* **A** *and* **I** *were obtained without contrast and the other images were obtained at these hourly intervals after intrathecal contrast administration (CT myelography), 0.5* **B**, **J**, *2* **C**, **K**, *4* **D**, **L**, *6* **E**, **M**, *8* **F**, **N**, *10* **G**, **O**, *22* **H**, **P** *h. The black arrowhead* **A** *indicates the syrinx. The myelogram dye concentration decreases more slowly from the subarachnoid space (***F***, black large arrow) before compared to after surgery (***N***, white arrowhead). Similarly, the dye concentration decreases more slowly in the syrinx before surgery (***H***, small black arrow) compared to after surgery (***P***, small white arrow).* **Q** *and* **R**, *Hounsfield units in this patient were measured in the spinal subarachnoid space (SAS), spinal cord (SC), and syrinx from the serial CT axial images and graphs were drawn of the mean and standard deviation of pixel values (error bars) in these regions of interest at each time point. The graphs confirm the visual impression that myelogram dye concentration decreases more slowly from the subarachnoid space before* **Q** *compared to after surgery* **R** *and that dye concentration decreases more slowly in the syrinx before surgery* **Q** *compared to after surgery* **R**.

patient had a communication between the fourth ventricle and the syrinx that was detectable on high-resolution MRI. The only significant difference in syrinx size among groups was that the anteroposterior width of the syringes was slightly smaller in the Ch-S group (6.2 mm) compared to the Sp-S (8.1 mm) and Tum-S (8.1 mm) groups ($P = .04$; $P = .05$, respectively; Table 1). The patient weights in the Ch-S, Sp-S, and the Tum-S groups were similar (80.2 ± 20.1, 80.7 ± 18.8, and 74.8 ± 20.9 kg, mean ± SD, respectively (Table 1)). At baseline, before injection of the contrast into the lumbar CSF, the HU in the syrinx was similar among groups (Ch-S, 14.3; Sp-S, 14.07; Tum-S, 16.2 [NS]; Figure 4A), as was the HU in the subarachnoid CSF at baseline.

In most patients and in group analysis, dye entry into the syrinx before surgery was significantly greater in Ch-S (Figures 1 and 4A) and Sp-S (Figures 2 and 4A) than with Tum-S (Figures 3 and 4A; see Table 2. In another measure of the accumulation of contrast in the syrinx, we calculated the area of HU under the concentration-time curve (AUC) in the syrinx over the first 10 h after contrast injection. This demonstrated greater accumulation of contrast in Ch-S and Sp-S compared to Tum-S (Figure 4B). Further, there was greater accumulation of contrast in the syrinx in patients before than after surgery (Ch-S, Sp-S; Table 2, Figure 4B).

The maximum concentration of contrast was consistently higher in the SAS than in the syrinx in all groups (Table 2). Since the effects of surgery for Ch-S and Sp-S are to eliminate the block of the free flow of CSF in the subarachnoid space at the level of the foramen magnum (Ch-S) or the site of localized arachnoid adhesions (Sp-S), we analyzed maximum HU in the SAS before and after surgery and the AUC of HU in the SAS before and after surgery (Table 2, Figures 4C and 4D). The AUC of the HU in the SAS was lower in patients with intramedullary tumor, who have no obstruction of the SAS, than in patients with obstructive lesions of the subarachnoid CSF associated with Ch-S or Sp-S (Table 2, Figure 4C). Maximum HU in the SAS after surgery was substantially less than before surgery in patients with Ch-S, but not in patients with Sp-S.

The cross-sectional areas of the syringes of each group were compared to see if lesser dye transport into tumor-related syringes was related to smaller syringes in the (Tum-S) group, but the opposite was the case when comparing Tum-S with Ch-S syringes, with Tum-S syringes having a larger cross-sectional area (38 ± 21) than Ch-S syringes (21 ± 12 mm^2, mean ± SD; $P = .02$). The difference between Sp-S (25 ± 24, mean ± SD) and Tum-S (38 ± 21 mm^2) was not statistically significant, however ($P = .10$).

DISCUSSION

Search for the origin of syrinx fluid in syringomyelia associated with the Chiari I malformation or with obstruction of the spinal CSF pathways by focal arachnoid adhesions below the foramen magnum has a long history. Gardner and Williams proposed that enlarged pressure waves or craniospinal pressure differentials forced CSF from the fourth ventricle and into the central canal of the spinal cord, distending the central canal until a syrinx cavity formed.[12-14] Subsequent autopsy and radiographic studies found that a patent central canal rarely occurs in adult patients with syringomyelia.[14,15] That none of the patients in our study had a connection between the fourth ventricle and the syrinx on MRI eliminates Gardner's or Williams' theories explaining the findings. Milhorat et al[16,17] proposed that a syrinx develops inferior to an obstructed central canal because ependymal hyperplasia occludes normal rostral flow of CSF in the central canal. Because obstruction of the central canal is the norm, rather than the exception, and because syringomyelia is rare, a syrinx should not occur solely from obstruction of the central canal, but would require excess fluid to be produced or transmitted to the center of the spinal cord.

Others argue that with Ch-S and Sp-S the syrinx fluid, the composition of which is identical to CSF,[18] derives by a mechanism external to the spinal cord, from subarachnoid CSF passing through the spinal cord and into the syrinx. Ball and Dayan[19] proposed that the tonsils obstruct the rapid upward movement of CSF from the spinal to the cranial subarachnoid space during episodic increases in thoracic venous pressure; thus, sporadic increased spinal subarachnoid pressure (during coughing, sneezing, and straining) pushes the CSF through the spinal cord along extracellular microscopic paths as the basis of

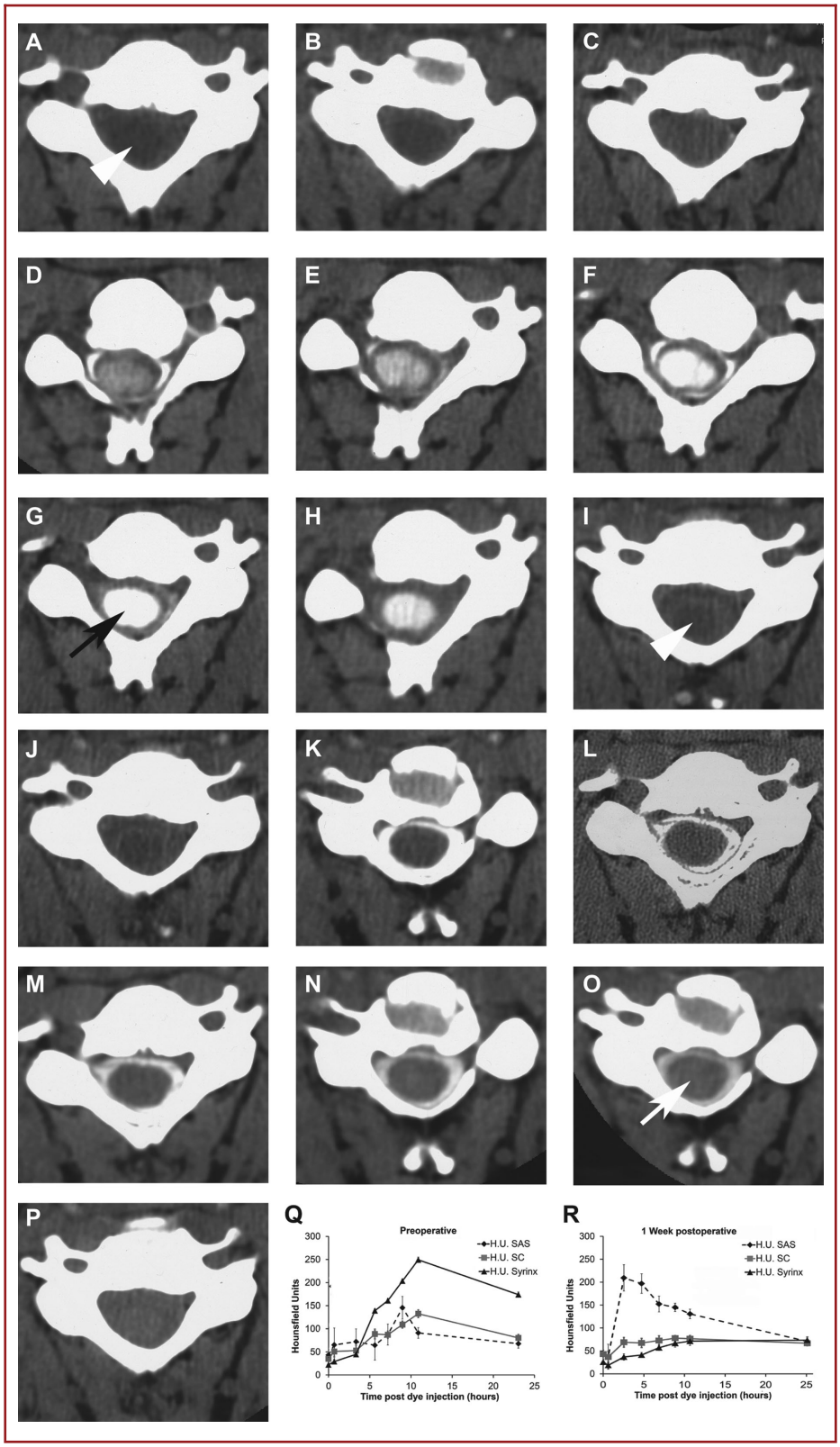
A
B
C
D
E
F
G
H
I
J
K
L
M
N
O
P
Q
Preoperative
H.U. SAS
H.U. SC
H.U. Syrinx
Hounsfield Units
Time post dye injection (hours)
R
1 Week postoperative
H.U. SAS
H.U. SC
H.U. Syrinx
Hounsfield Units
Time post dye injection (hours)

FIGURE 2. **A-P**, *Serial CT axial images at the C6 spinal segment before* **A** *through* **H** *and after* **I** *through* **P** *thoracic laminectomy and duraplasty in a patient with a history of instrumented fusion of a traumatic fracture dislocation at the T8-9 spinal level years before and subsequent development of post-traumatic syringomyelia (Sp-S). Images* **A** *and* **I** *were obtained without contrast and the other images were obtained at these intervals (hours) after intrathecal contrast administration (CT myelography), 0.6* **B**, **J**, *3* **C**, **K**, *5* **D**, **L**, *7* **E**, **M**, *9* **F**, **N**, *11* **G**, **O**, *23* **H**, **P** *h. The white arrowheads* **A**, **I** *indicate the central syrinx. Myelogram dye enters the syrinx to a much great extent before surgery (black arrow,* **G** *compared to after surgery (white arrow,* **O**. **Q** *and* **R**, *Hounsfield units in this patient were measured in the subarachnoid space, spinal cord, and syrinx from the sequential CT axial images, and graphs were drawn of the mean and standard deviation of pixel values (error bars) in these regions of interest at each time point. The graphs confirm the visual impression that much more myelogram dye enters the syrinx before* **Q** *compared to after* **R** *surgery in syringomyelia associated with a spinal canal lesion (Sp-S).*

the origin and progression of syringomyelia. They suggested that the same venous mechanism might underlie post-traumatic spinal syringomyelia. However, no studies demonstrate episodic venous pressure elevation transmitted to the spinal CSF as the underlying pathophysiology in syringomyelia, and it seems unlikely that these forces could produce the degree of movement of the contrast into the syrinx occurring over the 10-h interval in our study.

Oldfield et al[5] argued that elevated CSF pressure and pulse pressure in the subarachnoid space propel the CSF fluid through the Virchow-Robin spaces and the extracellular space of the spinal cord and into the syrinx. Swelling and edema of the spinal cord preceding the development of a syrinx supports the notion that transparenchymal passage of CSF from the SAS is an early step in the mechanism of syrinx formation.[20,21] Surgical relief of the obstructed CSF pathways reduces the size of the syrinx, prevents progression of myelopathy, and supports syringomyelia arising from outside the spinal cord.

Observations support the importance of abnormally high subarachnoid CSF systolic pressure waves in this process. Early CT myelographic studies showed that CSF containing ionic and nonionic contrast media passes from the subarachnoid space to the syrinx.[22] Further, intrathecal radioactive tracer studies in patients demonstrate transmural flow from the subarachnoid space into the syrinx.[23,24] Under physiological conditions CSF moves into the spinal cord under the combined forces of diffusion and convection (bulk flow). Studies using low molecular weight tracers and performed under normal physiological conditions concluded that the movement of the molecules into the spinal cord occurs via diffusion.[25,26] The earliest studies performed under normal physiological conditions were with intrathecal injection of macromolecular tracers and examination of postmortem histology. Brierley demonstrated penetration of horseradish peroxidase (particle size, 0.5 um) into the rabbit spinal cord along the perivascular spaces reaching the central canal, deeper than could occur from diffusion alone with macromolecules.[27] Lee and Olszewski made similar observations, using radiolabeled albumen.[28] Rennels et al[29] examined this further and demonstrated that the penetration of horseradish peroxidase from the subarachnoid space and deep into the perivascular spaces of the spinal cord, brainstem, and brain depends on the existence of pulse pressure, as the penetration was substantially reduced by constriction of the brachiocephalic artery and reduction of the intracranial pulse pressure in dogs. Stoodley et al[30] subsequently demonstrated that horseradish peroxidase penetrated to the central canal of the spinal cord of sheep after intrathecal injection, but this did not occur after dampening the arterial pulsations by partially ligating the brachiocephalic trunk. Thus, small and large molecules move into the spinal cord from without by the combined forces of diffusion and bulk flow facilitated by pulse pressure in the CSF. This was the basis of our proposal that the exaggerated absolute pressure and pulse pressure in the subarachnoid space is an important component of the development and progression of syringomyelia with Ch-S and Sp-S.[2-5]

In contrast, syringes associated with intramedullary hemangioblastomas and cerebellar cysts associated with hemangioblastomas arise from the excess vascular permeability of the tumor vessels and vasogenic edema fluid containing high levels of protein passing from the intramedullary tumor directly into the spinal cord from within.[6,7] Noninvasive MRI techniques demonstrated transport of intravascular contrast from cerebellar hemangioblastomas to peritumoral cysts.[7] In the current study, syringomyelia with intramedullary tumors acts as a control for movement of the low molecular weight contrast into syrinx under normal physiological circumstance of the unobstructed SAS. Note the increase in HU in the syrinx after intrathecal contrast injection in all groups (Figure 4A). The differences measured between groups are consistent with our hypothesis, as there were substantial and significant differences in almost all the comparisons in the analysis. The higher penetration of the contrast into the syrinx of Ch-S and Sp-S patients resulted from enhanced bulk flow of CSF through the cord and into the syrinx driven by the increased subarachnoid CSF absolute pressure and pulse pressures, previously demonstrated in these patient groups, since the passage of contrast into the syrinx was reduced by removing the subarachnoid CSF obstruction, which eliminates the excess subarachnoid CSF pressures.[2,3,5] One could speculate that higher syringeal pressure in the intramedullary tumor group than other groups prevented convective bulk flow of dye from the subarachnoid space to intramedullary tumor-associated syringes. Lower subarachnoid dye concentrations in the intramedullary group would also reduce the amount of dye passing from the subarachnoid space to the syrinx.

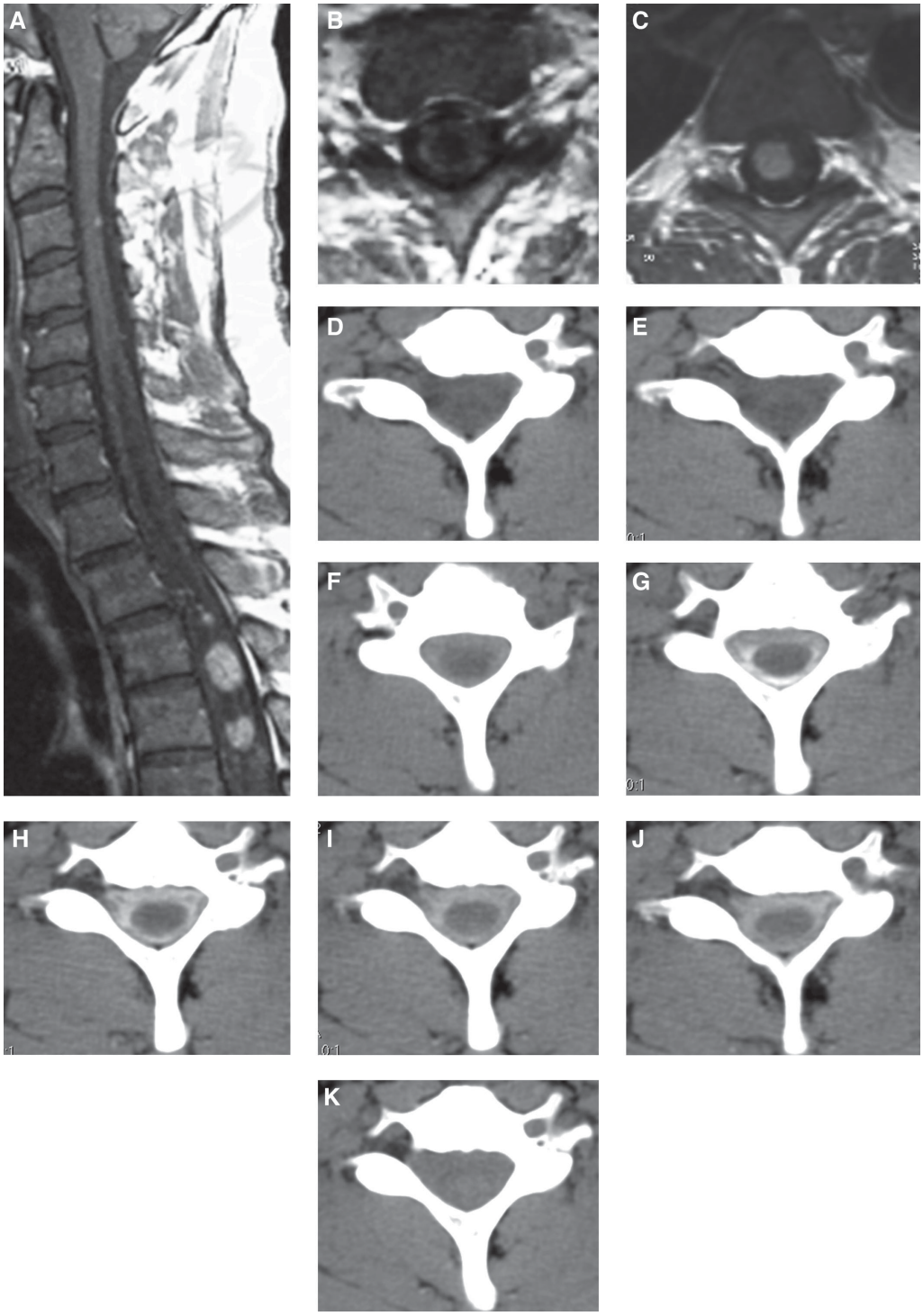

FIGURE 3. *T1-weighted MRI scan of the cervical spine after intravenous gadolinium contrast administration in a middle-aged man with von Hippel-Lindau disease demonstrates a syrinx on midsagittal (**A**, white arrowhead) and axial (**B**, white arrowhead) images adjacent to an enhancing intramedullary hemangioblastoma (**C**, black arrow). Serial CT imaging was performed, before **D** and after **E** through **K** intrathecal installation of contrast. Contrast dye is seen around the spinal cord in the subarachnoid space, **F** through **J** but not in the syrinx.*

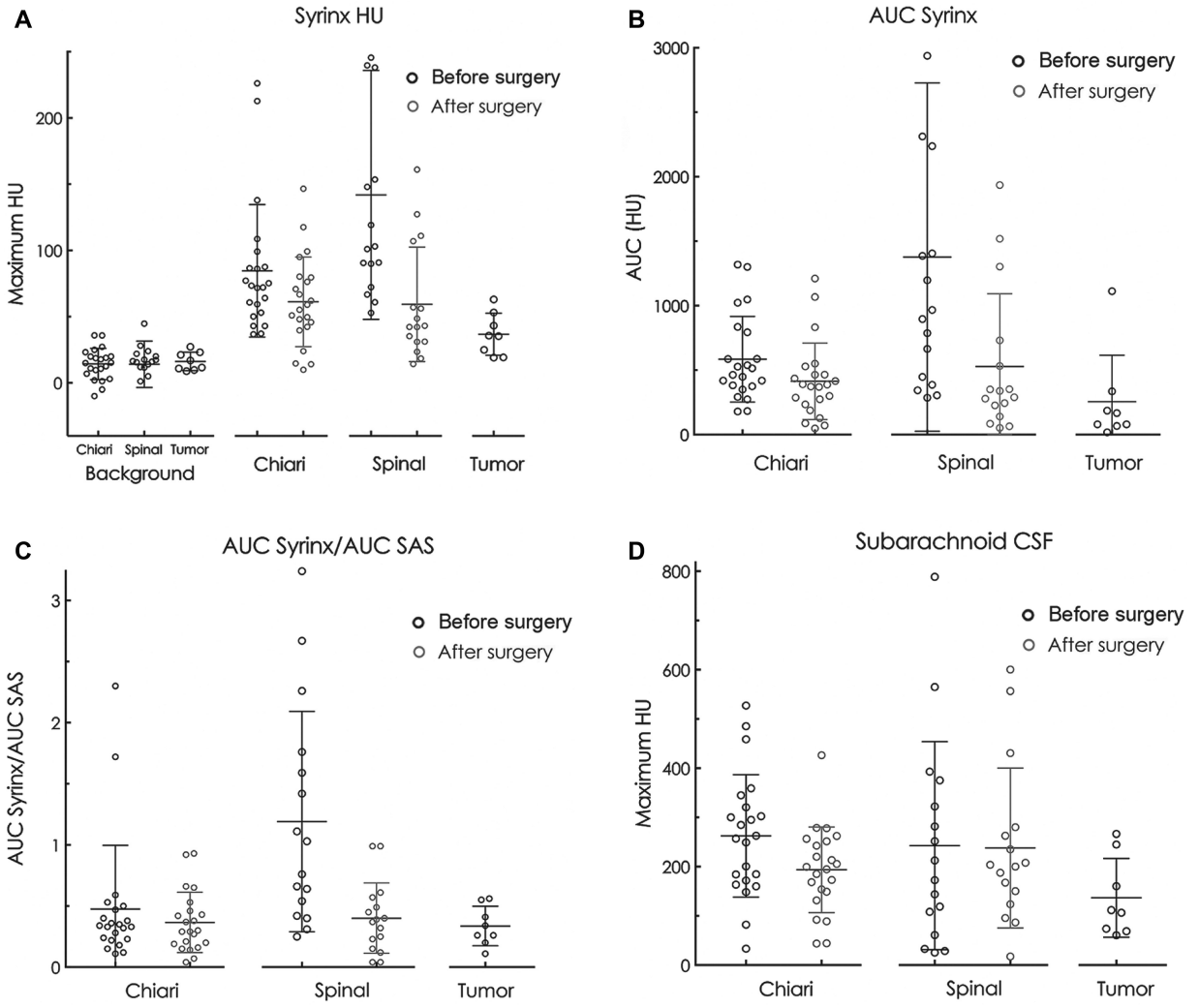

FIGURE 4. *Graphical representation of group results.* **A**, *The baseline HU of the syrinx before intrathecal contrast injection was similar among groups. The maximum HU in the syrinx after intrathecal contrast injection minus the baseline values is shown for each group, including the values after surgery for the Chiari and spinal syringomyelia groups. Two points are off the graph (–40.5 in the spinal baseline group, 399 in the spinal group before surgery).* **B**, *The area of HU under the concentration-time curve (AUC) in the syrinx was greater in the Chiari and spinal groups than the tumor group and was greater before compared to after surgery. One point is off the graph, 3412 in the Chiari group before surgery.* **C**, *The ratios of the AUC between the syrinx and subarachnoid CSF were greater in the Chiari and spinal groups compared to the tumor group, but returned to values like the tumor group after surgical decompression of the subarachnoid CSF obstruction.* **D**, *Mean maximum HU in the spinal subarachnoid CSF before surgery was greater in the Chiari and spinal group than the tumor group before surgery and was reduced by surgery in the Chiari, but not the spinal group. Each circle represents 1 patient. The long horizontal lines indicate the mean for each group. The shorter horizontal lines indicate 1 SD above and below the mean.*

Another physiological abnormality common to Chiari I malformations and SAS obstruction-related syringomyelia is partial entrapment of the spinal CSF compartment with reduced compliance of the spinal CSF space.[2,3,5] Since patients with increased intracranial pressure and pulse pressure with hydrocephalous, pseudotumor cerebri, and tumors, patients who do not have occlusion of the subarachnoid CSF, do not get syringomyelia, the block of free flow of CSF in the SAS is required for the development of syringomyelia. Craniocervical decompression and duraplasty effectively resolves Chiari I-related syringomyelia because opening the CSF pathways at the foramen magnum eliminates the force that drives CSF into the spinal cord.[2,4,5] SAS obstruction-related syringomyelia similarly responds to surgical opening of obstructed CSF pathways.[3,31] Note the significantly higher AUC syrinx/AUC SAS before surgery in the Sp-S group than in the Tum-S group (Table 2,

TABLE 1. Syrinx Sizes and Body Weight

	Chiari I Mean before surgery	Spinal subarachnoid space obstruction-related syringomyelia (spinal) Mean before surgery	Intramedullary tumor Mean before surgery	Comparison Chiari to tumor before surgery *P* value	Comparison spinal to tumor before surgery *P* value	Comparison Chiari to spinal before surgery *P* value
Syrinx anteroposterior width (mm)	6.2 (2.4)	8.1 (3.0)	8.1 (2.2)	.05*	.99	.04**
Syrinx lateral width (mm)	6.8 (2.0)	6.5 (1.8)	6.4 (2.8)	.60	.94	.54
Syrinx length (cm)	18.4 (9.9)	22.4 (11.1)	16.1 (11.6)	.58	.21	.26
Syrinx length (segments)	11.1 (5.3)	11.7 (5.0)	9.1 (5.2)	.34	.24	.73
Body weight (kg)	80.2 (20.1)	80.7 (18.8)	74.8 (20.9)	.50	.48	.93

Comparisons between groups are with the unpaired *t* test (Mann-Whitney).
Values are mean (standard deviation).
*Statistically significant difference.

TABLE 2. Contrast Radiodensity in Hounsfield Units (HU) Measured in the Subarachnoid Space and Syrinx

	Chiari I			Spinal subarachnoid space obstruction-related syringomyelia (spinal)			Intramedullary tumor	Comparison Chiari to tumor before surgery	Comparison spinal to tumor before surgery	Comparison Chiari to spinal before surgery
	Mean before surgery	Mean after surgery	Comparison before vs after surgery	Mean before surgery	Mean after surgery	Comparison before vs after surgery	Mean	*P* value	*P* value	*P* value
Maximum HU syrinx-baseline HU	84.2 (50.0)	61.2 (33.8)	0.03	141.9 (94.0)	59.3 (43.2)	0.0001	36.7 (15.9)	.0002	.0001	.003
Maximum - baseline subarachnoid CSF HU	262.5 (124.4)	193.6 (87.0)	0.02	242.6 (211.2)	237.9 (162.5)	0.9	136.7 (80.1)	.004	.2	.2
HU AUC syrinx	584.3 (331.8)	413.9 (296.9)	0.004	1377 (1351)	527.7 (564.5)	0.002	255.6 (359.8)	.001	.0005	.04
AUC HU subarachnoid CSF	1691 (791)	1288 (658)	0.02	1593 (1314)	1235 (600)	0.8	643.8 (602.5)	.002	.02	.4
HU AUC syrinx/HU AUC subarachnoid CSF	0.48 (0.52)	0.37 (0.25)	0.4	1.19 (0.9)	0.40 (0.29)	0.0008	0.34 (0.16)	.9	.003	.0004

HU AUC, area of the concentration in HU under the concentration/time curve.
Comparisons between groups are with the unpaired *t* test (Mann-Whitney).
Comparisons within groups before vs. after surgery are with paired *t* test.
Values are mean (standard deviation).

Figure 4C), as well as the drop in the maximum AUC of HU in the SAS after surgery to eliminate the subarachnoid obstruction in patients with Chiari I malformation (Figure 4D), indicating increased clearance of the dye from the subarachnoid space as a result of the surgery. Lower subarachnoid dye concentrations in the intramedullary group could have reduced dye transit from the subarachnoid space to the syrinx in this group.

In animal models of syringomyelia, subarachnoid CSF enters the spinal cord through enlarged Virchow-Robin (periarterial) spaces that surround the segmental vascular supply of the spinal cord.[19,32,33] Based on computer modeling, it has been proposed that in syringomyelia spinal cord arterial pulsations in the Virchow-Robin spaces pump CSF into the spinal cord.[34,35] However, in the current study the passage of dye into the syrinx was reduced and the syrinx subsequently disappeared by simply eliminating the obstruction of the subarachnoid CSF, surgery which does not alter the arterial pressure or arterial pulsations of the spinal cord vessels.

Patients in this study with the congenital tumor syndrome, von Hippel-Lindau disease, developed intramedullary hemangioblastoma and syringomyelia. Genetics factors predisposing to inheritance of Chiari I malformation or adhesive arachnoiditis may also lead to syringomyelia.[36,37] Syringomyelia from loss of ependymal cell ciliary function in the spinal central canal has not been reported, but loss of ependymal cell ciliary function in the ventricular system was associated with hydrocephalus and scoliosis in zebrafish protein tyrosine kinase-7 mutants.[38]

CONCLUSION

The findings of this study are consistent with the hypothesis and the results of previous studies on the origin and progression of syringomyelia.[2-5] Normally, CSF is displaced from the basal cisterns of the intracranial cavity, through the foramen magnum, and into the more-compliant spinal canal to compensate for increases in brain arterial volume during cardiac systole. However, in patients with Ch-S, the cerebellar tonsils obstruct CSF displacement across the foramen magnum, so pulsatile changes in brain arterial volume during the cardiac cycle create increased intracranial pulse pressure waves and brain pulsation, which is transmitted through the piston-like action of the cerebellar tonsils to the SAS as an enlarged pulse pressure wave. Increased subarachnoid pulse pressure initiates a syrinx by driving CSF through the perivascular spaces and into the spinal cord, and promotes syrinx progression by acting on the surface of the spinal cord to create longitudinal oscillation of syrinx fluid during the cardiac cycle. The same mechanism occurs with SAS obstruction-related syringomyelia, the obstruction to the free flow of CSF in the subarachnoid space just occurs at a lower level, also producing abnormally high CSF pressure waves that force CSF into the spinal cord from without.[3] This concept is supported by anatomic and physiological data from prior studies.[2-4]

Disclosures

The study was funded by the Intramural Research Program of National Institute of Neurological Disorders and Stroke at the National Institutes of Health. The authors have no personal, financial, or institutional interest in the drugs, materials, or devices described in this article.

REFERENCES

1. Sobel DF, Barkovich AJ, Munderloh SH. Metrizamide myelography and postmyelographic computed tomography: comparative adequacy in the cervical spine. *Science*. 1984;5(4):1341-1344.
2. Heiss JD, Patronas N, DeVroom HL, et al. Elucidating the pathophysiology of syringomyelia. *J Neurosurg*. 1999;91(4):553-562.
3. Heiss JD, Snyder K, Peterson MM, et al. Pathophysiology of primary spinal syringomyelia. *J Neurosurg Spine*. 2012;17(5):367-380.
4. Heiss JD, Suffredini G, Smith R, et al. Pathophysiology of persistent syringomyelia after decompressive craniocervical surgery. Clinical article. *J Neurosurg Spine*. 2010;13(6):729-742.
5. Oldfield EH, Muraszko K, Shawker TH, Patronas NJ. Pathophysiology of syringomyelia associated with Chiari I malformation of the cerebellar tonsils. Implications for diagnosis and treatment. *J Neurosurg*. 1994;80(1):3-15.
6. Lonser RR, Heiss JD, Oldfield EH. Syringomyelia, hemangioblastomas, and Chiari I malformation. Case illustration. *J Neurosurg*. 1999;90(1):169.
7. Lonser RR, Vortmeyer AO, Butman JA, et al. Edema is a precursor to central nervous system peritumoral cyst formation. *Ann Neurol*. 2005;58(3):392-399.
8. Hindmarsh T. Elimination of water-soluble contrast media from the subarachnoid space. Investigation with computer tomography. *Acta Radiol Suppl*. 1975;346:45-49.
9. Benzel EC, Chesson AL. Computed tomography number correlations for metrizamide computed tomographic ventriculography. *Surg Neurol*. 1987;27(2):126-130.
10. Wetjen NM, Heiss JD, Oldfield EH. Time course of syringomyelia resolution following decompression of Chiari malformation Type I. *J Neurosurg Pediatr*. 2008;1(2):118-123.
11. Lonser RR, Weil RJ, Wanebo JE, DeVroom HL, Oldfield EH. Surgical management of spinal cord hemangioblastomas in patients with von Hippel-Lindau disease. *J Neurosurg*. 2003;98(1):106-116.
12. Gardner WJ, Angel J. The mechanism of syringomyelia and its surgical correction. *Clin Neurosurg*. 1958;6:131-140.
13. Williams B. The distending force in the production of communicating syringomyelia. *Lancet*. 1969;2(7622):696-697.
14. Williams B. Syringomyelia. *Neurosurg Clin N Am*. 1990;1(3):653-685.
15. Foster JB, Hudgson P. The pathology of communicating syringomyelia. In: Barnett HJM, Foster JB, Hudgson P, eds. *Syringomyelia*. Vol 1. Philadelphia: W. B. Saunders Company, Ltd; 1973:79-103.
16. Milhorat TH, Miller JI, Johnson WD, Adler DE, Heger IM. Anatomical basis of syringomyelia occurring with hindbrain lesions. *Neurosurgery*. 1993;32(5):748-754; discussion 754.
17. Milhorat TH, Nobandegani F, Miller JI, Rao C. Noncommunicating syringomyelia following occlusion of central canal in rats. Experimental model and histological findings. *J Neurosurg*. 1993;78(2):274-279.
18. Hankinson J. Syringomyelia and the surgeon. *Mod Trends Neurol*. 1970;5:127-148.
19. Ball MJ, Dayan AD. Pathogenesis of syringomyelia. *Lancet*. 1972;2(7781):799-801.
20. Fischbein NJ, Dillon WP, Cobbs C, Weinstein PR. The "presyrinx" state: a reversible myelopathic condition that may precede syringomyelia. *AJNR Am J Neuroradiol*. 1999;20(1):7-20.
21. Levy EI, Heiss JD, Kent MS, Riedel CJ, Oldfield EH. Spinal cord swelling preceding syrinx development. Case report. *J Neurosurg*. 2000;92(1 Suppl):93-97.
22. Li KC, Chui MC. Conventional and CT metrizamide myelography in Arnold-Chiari I malformation and syringomyelia. *AJNR Am J Neuroradiol*. 1987;8(1):11-17.
23. Ellertsson AB, Greitz T. Myelocystographic and fluorescein studies to demonstrate communication between intramedullary cysts and the cerebrospinal fluid space. *Acta Neurol Scand*. 1969;45(4):418-430.

24. Greitz T, Ellertsson AB. Isotope scanning of spinal cord cysts. *Acta Radiol Diagn (Stockh)*. 1969;8(4):310-320.
25. Dubois PJ, Drayer BP, Sage M, Osborne D, Heinz ER. Intramedullary penetrance of metrizamide in the dog spinal cord. *AJNR Am J Neuroradiol*. 1981;2(4):313-317.
26. Fenstermacher JD, Bradbury MW, du Boulay G, Kendall BE, Radu EW. The distribution of 125I-metrizamide and 125I-diatrizoate between blood, brain and cerebrospinal fluid in the rabbit. *Neuroradiology*. 1980;19(4):171-180.
27. Brierley JB. The penetration of particulate matter from the cerebrospinal fluid into the spinal ganglia, peripheral nerves, and perivascular spaces of the central nervous system. *J Neurol Neurosurg Psychiatry*. 1950;13(3):203-215.
28. Lee JC, Olszewski J. Penetration of radioactive bovine albumin from cerebrospinal fluid into brain tissue. *Neurology*. 1960;10(9):814-822.
29. Rennels ML, Blaumanis OR, Grady PA. Rapid solute transport throughout the brain via paravascular fluid pathways. *Adv Neurol*. 1990;52:431-439.
30. Stoodley MA, Jones NR, Brown CJ. Evidence for rapid fluid flow from the subarachnoid space into the spinal cord central canal in the rat. *Brain Res*. 1996;707(2):155-164.
31. Klekamp J, Batzdorf U, Samii M, Bothe HW. The surgical treatment of Chiari I malformation. *Acta Neurochir (Wien)*. 1996;138(7):788-801.
32. Hassin GB. A contribution to the histopathology and histogenesis of syringomyelia. *Arch Neurol Psych*. 1920;3(2):130-146.
33. Ikata T, Masaki K, Kashiwaguchi S. Clinical and experimental studies on permeability of tracers in normal spinal cord and syringomyelia. *Spine*. 1988;13(7):737-741.
34. Bilston LE, Stoodley MA, Fletcher DF. The influence of the relative timing of arterial and subarachnoid space pulse waves on spinal perivascular cerebrospinal fluid flow as a possible factor in syrinx development. *J Neurosurg*. 2010;112(4):808-813.
35. Bilston LE, Fletcher DF, Brodbelt AR, Stoodley MA. Arterial pulsation-driven cerebrospinal fluid flow in the perivascular space: a computational model. *Comput Methods Biomech Biomed Engin*. 2003;6(4):235-241.
36. Milhorat TH, Chou MW, Trinidad EM, et al. Chiari I malformation redefined: clinical and radiographic findings for 364 symptomatic patients. *Neurosurgery*. 1999;44(5):1005-1017.
37. Pasoglou V, Janin N, Tebache M, Tegos TJ, Born JD, Collignon L. Familial adhesive arachnoiditis associated with syringomyelia. *AJNR Am J Neuroradiol*. 2014;35(6):1232-1236.
38. Grimes DT, Boswell CW, Morante NFC, Henkelman RM, Burdine RD, Ciruna B. Zebrafish models of idiopathic scoliosis link cerebrospinal fluid flow defects to spine curvature. *Science*. 2016;352(6291):1341-1344.

COMMENT

The authors of this study assessed the accumulation of myelogram dye following lumbar instillation in a group of patients with syringomyelia of various etiologies. The purpose of the study was to determine the source of the cerebrospinal fluid within the syrinx and how different etiologies differed in the communication between the spinal subarachnoid space and the syrinx itself. Three groups were studied including syringomyelia related to Chiari I malformation, that related to restriction of spinal fluid flow in the spinal subarachnoid space and finally syringomyelia secondary to intramedullary spinal cord tumors. The patients obtained computerized tomographic studies through the area of maximum distension of the spinal cord at intervals from 30 minutes to 2 hours for 22 hours and measured the rate of flow and clearance of dye in the syrinx cavity. Both the Chiari-related and flow-related syringes showed similar rates of penetration and clearance while the penetration of the dye into the syrinx in the case of the intramedullary tumors was much slower. Postoperative studies were performed in patients with Chiari related and flow related syringes. These showed that the penetration of dye was significantly lessened in the Chiari related patients than in the patients with obstruction to flow in the spinal subarachnoid spaces.

Recognizing where the cerebrospinal fluid (CSF) comes from and how it gets out leads to a better understanding of the causation and treatment of the condition.[1,2]

What can be inferred from this work? The authors discuss the theories of pathogenesis of syringomyelia as it relates to the filling of the syrinx. Most of this discussion and indeed much of the research relates to the relationship of cerebellar tonsilar herniation with the development of syringomyelia. The findings of this study support the work of previous authors showing that the source of the CSF in the syrinx is mainly related to flow from the spinal subarachnoid space to the syrinx. This can be due to increase of transient waves forcing fluid into the parenchyma of the spinal cord via the Virchow-Robin spaces. These waves may relate to augmentation of cardiac pulses or to transients created by Valsalva maneuvers.[3] The study here implies that blockage of the spinal subarachnoid space would have essentially the same effect due to decrease in compliance of the subarachnoid space. In both instances, it is likely that there is a transmantle gradient between the syrinx cavity and the spinal subarachnoid space forcing the fluid to flow through the parenchyma into the syrinx cavity causing the syrinx to expand. If there is a complete obliteration of the central canal then the spinal cord becomes distended with extracellular fluid creating the "pre-syrinx" state.

The authors identified 6 of 16 patients with failure of flow in the spinal subarachnoid spaces who had trauma as a causative event. The authors do not spedcify whether or not these patients had spinal cord injuries as part of the pathology. Traumatic syrinxes are a completely different entity and I will assume that none of these patients had suffered from true traumatic syrinxes.

The third group of syrinx patients studied here are patients with syringes secondary to intramedullary spinal cord tumors. The patients who have been studied are specifically patients with von Hippel Lindau syndrome and all the tumors were hemangioblastomas. The study showed quite convincingly that the CSF within the syrinx was produced within the tumor spinal cord itself. There is significant evidence that this particular tumor is associated with cysts whether they be in the brain or in the spinal cord. The tumor itself can be the likely source for the CSF within the cysts due to the vascular basis of the tumor seemingly similar to choroid plexus.[4] The tumors cause not only obstruction of flow of CSF from the spinal cord to the point of emptying into the fourth ventricle but also inhibit flow within the white matter parenchyma of the spinal cord. Syrinx related to intramedullary gliomas and ependymomas were not studied but neither of these tumors have been shown to have the abilty to produce CSF. It is likely then that the source of the CSF in this condition relates to the creation of CSF as a byproduct of spinal cord metabolism similar to the production of CSF from the brain parenchyma following choroid plexectomies. Since the mass of the spinal cord is much smaller than that of the brain it is likely that the production of intra-syrinx CSF would be quite slow.[5]

The most important take-home message here relates to the management of the syrinx associated with flow restriction of the spinal subarachnoid space. This has been called "primary spinal syringomyelia." The identification of the source of the CSF is from the spinal subarachnoid space lead to a focus of management from actual opening of the spinal cord or shunting the syrinx to reestablishing flow within the spinal subarachnoid space. Actual opening of the spinal cord for drainage

is rarely effective on its own and shunting of the syrinx can be problematic leading to symptomatic tethering of the spinal cord.[6]

Harold L. Rekate
Great Neck, New York

1. Heiss JD, Patronas N, DeVroom HL, Shawker T, Ennis R, Kammerer W et al. Elucidating the pathophysiology of syringomyelia. *J Neurosurg*. 1999;91(4):553-62.
2. Heiss JD, Snyder K, Peterson MM, Patronas NJ, Butman JA, Smith RK et al. Pathophysiology of primary spinal syringomyelia. *J Neurosurg Spine*. 2012;17(5):367-80.
3. Oldfield EH, Muraszko K, Shawker TH, Patronas NJ. Pathophysiology of syringomyelia associated with Chiari I malformation of the cerebellar tonsils. Implications for diagnosis and treatment. *J Neurosurg*. 1994;80(1):3-15.
4. Lonser RR, Heiss JD, Oldfield EH. Syringomyelia, hemangioblastomas, and Chiari I malformation. Case illustration. *J Neurosurg*. 1999;90(1):169.
5. Rekate H. Syringomyelia in children. In:Batjer HHL, C, eds. *Texttbook of Neurologic Surgery*. Baltimore: Lippincott, williams and Wilkins; 2002. p. 960-6.
6. Smith KA, Rekate HL. Delayed postoperative tethering of the cervical spinal cord. *J Neurosurg*. 1994;81(2):196-201.

Jeff kept painting, refining his style and techniques. He donated art to charity fundraisers, like the Medical Missions Foundation Gala in 2007. He began receiving commissions from people who had seen his art or heard his story; from his ophthalmologist, from his favorite eye glasses company, from a local apartment complex, on it went. At age 17, Jeff sold $140 000 in art and generated another $200 000 for charity through canvas donations. In 2010, he was named global ambassador for the Make-A-Wish® Foundation (he continued to donate to their fundraising auctions, giving back to those who granted his wish). In 2011, Prudential gave Jeff one of the 10 national Prudential Spirit of Community Awards. In 2012, Jeff was selected as the United States Small Business Administration's Region VII Young Entrepreneur of the Year. Image: *Arriving in Murano* © Jeffrey Owen Hanson LLC. Used with permission, all rights reserved.